frontiers | Frontiers in Fungal Biology

TYPE Original Research
PUBLISHED 27 June 2023
DOI 10.3389/ffunb.2023.1201889

OPEN ACCESS

EDITED BY
Xiaoyun Su,
Chinese Academy of Agricultural Sciences (CAAS), China

REVIEWED BY
Jiwei Zhang,
University of Minnesota Twin Cities, United States
Rakesh Kumar Sharma,
Manipal University Jaipur, India

*CORRESPONDENCE
Hirofumi Hirai
hirai.hirofumi@shizuoka.ac.jp

RECEIVED 07 April 2023
ACCEPTED 05 June 2023
PUBLISHED 27 June 2023

CITATION
Mori T, Takahashi S, Soga A, Arimoto M, Kishikawa R, Yama Y, Dohra H, Kawagishi H and Hirai H (2023) Aerobic H_2 production related to formate metabolism in white-rot fungi.
Front. Fungal Biol. 4:1201889.
doi: 10.3389/ffunb.2023.1201889

Aerobic H_2 production related to formate metabolism in white-rot fungi

Toshio Mori[1,2], Saaya Takahashi[1], Ayumi Soga[1], Misa Arimoto[1], Rintaro Kishikawa[1], Yuhei Yama[1], Hideo Dohra[2,3,4,5], Hirokazu Kawagishi[1,2] and Hirofumi Hirai[1,2,4]*

[1]Faculty of Agriculture, Shizuoka University, Shizuoka, Japan, [2]Research Institute for Mushroom Science, Shizuoka University, Shizuoka, Japan, [3]Faculty of Science, Shizuoka University, Shizuoka, Japan, [4]Research Institute of Green Science and Technology, Shizuoka University, Shizuoka, Japan, [5]Graduate School of Science and Technology, Shizuoka University, Shizuoka, Japan

Biohydrogen is mainly produced by anaerobic bacteria, anaerobic fungi, and algae under anaerobic conditions. In higher eukaryotes, it is thought that molecular hydrogen (H_2) functions as a signaling molecule for physiological processes such as stress responses. Here, it is demonstrated that white-rot fungi produce H_2 during wood decay. The white-rot fungus *Trametes versicolor* produces H_2 from wood under aerobic conditions, and H_2 production is completely suppressed under hypoxic conditions. Additionally, oxalate and formate supplementation of the wood culture increased the level of H_2 evolution. RNA-seq analyses revealed that *T. versicolor* oxalate production from the TCA/glyoxylate cycle was down-regulated, and conversely, genes encoding oxalate and formate metabolism enzymes were up-regulated. Although the involvement in H_2 production of a gene annotated as an iron hydrogenase was uncertain, the results of organic acid supplementation, gene expression, and self-recombination experiments strongly suggest that formate metabolism plays a role in the mechanism of H_2 production by this fungus. It is expected that this novel finding of aerobic H_2 production from wood biomass by a white-rot fungus will open new fields in biohydrogen research.

KEYWORDS
aerobic H_2 production, formate dehydrogenase, oxalate metabolism, *Trametes versicolor*, white-rot fungi

1 Introduction

Hydrogen gas is considered a potential sustainable energy carrier due to its advantages of high energy density, zero emissions when burning, and ease of production from various renewable sources. H_2 can be produced from biomass materials *via* both thermochemical and biological processes. Photo- and dark fermentation are biological conversion processes by which organic substrates and/or biomass materials can be used to produce H_2 by a diverse group of microorganisms. In dark fermentation, carbohydrates in the biomass are

broken anaerobically to H_2, CO_2, and organic acids by hydrogen-producing anaerobes (Ghimire et al., 2015). Some anaerobic bacteria, such as those of the genera *Escherichia* and *Clostridium*, can produce H_2 from organic acids (Mnatsakanyan et al., 2004; Matsumoto and Nishimura, 2007). Photo-fermentation of organic substrates is performed by photosynthetic bacteria. These bacteria utilize small organic acids to produce H_2 under anaerobic conditions in the presence of light (Azwar et al., 2014). Various anaerobic eukaryotes are also able to produce H_2 in hydrogenosomes. The anaerobic fungi *Neocallimastix* and *Piromyces* spp. are well-known H_2 producers (Hackstein et al., 1999). These enteric fungi hydrolyze carbohydrates, and the resulting sugars are metabolized to pyruvate *via* glycolysis or to malate *via* the tricarboxylic acid (TCA) cycle (Hess et al., 2020). Hydrogenosomes metabolize pyruvate and malate to acetate for ATP generation, and H_2 and CO_2 are also generated by the combined ATP generation reaction (Marvin-Sikkema et al., 1993; Hackstein et al., 1999). Organic acids often function as important factors in the H_2 production process in anaerobes.

Although hydrogenase-like (or NARF; nuclear prelamin A recognition factor, NAR1; cytosolic Fe-S cluster assembly factor) genes are widely distributed in the genomes of higher eukaryotes, their function and role remain unknown (Horner et al., 2002). It is generally thought that animal cells are unable to generate H_2, but it is also known that molecular hydrogen has diverse biological effects in animals, including anti-oxidative stress, anti-inflammatory, and anti-allergic effects (Ohta, 2012). Higher plants are also affected by H_2, as it improves tolerance to various abiotic stresses, including oxidative, salt, and desiccation stress (Li et al., 2018). Additionally, it is thought that H_2 improves physiological processes such as growth and development in higher plants and interacts other signaling molecules. Some early studies demonstrated hydrogenase-mediated H_2 production in seedlings of some higher plants under sterile conditions (Renwick et al., 1964; Torres et al., 1986). Some recent reports indicated that plant hormones and abiotic stresses promote endogenous H_2 release in higher plants and that H_2 signaling induces plant antioxidant defenses and enhances salt tolerance (Xie et al., 2012; Zeng et al., 2013). Although details of the H_2 production and H_2 signaling pathways remain unclear, molecular H_2 seems to play a very important role in stress responses in higher eukaryotes.

White-rot fungi are unique microorganisms that are capable of degrading all main wood components, cellulose, hemicellulose, and lignin. During lignin degradation, white-rot fungi produce various reactive oxygen species (ROS) and radicals, such as radical mediators (Dashtban et al., 2010). White-rot fungi also produce oxalate to release and mineralize excessive carbon in order to grow on woody materials that have an extremely high C/N ratio (Shimada et al., 1994). Based on these data, the authors predicted that white-rot fungi, which are always exposed to oxidative stress during wood decay and have excellent ability to metabolize organic acids, can produce H_2 in conjunction with organic acid metabolism to enhance oxidative stress tolerance. In this study, it was evaluated the H_2 production ability of various white-rot fungi during wood decay and investigated the underlying production mechanism.

2 Materials and methods

2.1 Fungal strains

White-rot fungi, *Pleurotus ostreatus* NBRC 33211, NBRC 104981, *Trametes hirsuta* NBRC 104984, NBRC 106840, and *Trametes versicolor* NBRC 104985, NBRC 106839 were obtained from the National Institute of Technology and Evaluation, Japan. *Phanerochaete chrysosporium* ME-446 (ATCC 34541) and *Phanerochaete sordida* YK-624 (ATCC 90872) were obtained from the American Type Culture Collection, USA. *Ceriporia lacerata* K-70 (accession number [AN] of internal transcribed sequence [ITS]: LC312413), *Phanerochaete* sp. K-64 (AN-ITS: LC710144), K-91 (AN-ITS: LC710143), K-97-2 (AN-ITS: LC710142), M-4 (AN-ITS: LC710145), *Schizophyllum commune* M-21 (AN-ITS: LC710146), *T. hirsuta* M-9 (AN-ITS: LC710150), *T. versicolor* K-39 (AN-ITS: LC710147), K-41 (AN-ITS: LC312415), K-86 (AN-ITS: LC710148), M-24 (AN-ITS: LC710149) and unidentified K-89 were isolated from naturally decaying wood samples and identified based on their ITS, following a previous report (Mori et al., 2018).

2.2 Test of H_2 evolution from wood meal

All fungal strains were grown on PDA at 30°C. Two mycelial discs (10 mm diameter) were punched from the edge of the mycelia and placed into a 70-mL serum vial containing 0.5 g of extractive-free beech or cedar wood meal (80-100 mesh, moisture content: 80%). After 5 days of pre-incubation at 30°C under atmospheric pressure, the inoculated vial was sealed with a butyl rubber plug to limit the O_2 supply and prevent H_2 diffusion. The sealed vial was incubated for 14 days at 30°C, and then the headspace gas was sampled, and H_2 production was analyzed by gas chromatography on an instrument equipped with a thermal conductivity detector (GC-TCD), as previously reported (Mori et al., 2016).

2.3 Characterization of H_2 production activity of *T versicolor* K-41

To elucidate the relationship between O_2 and H_2 production by *T. versicolor* K-41, the experiments described below were performed. First, 5-day pre-cultures of *T. versicolor* K-41 on 0.5 g of cedar wood meal (80-100 mesh, moisture content: 80%) in serum vials were incubated stationary at 30°C after sealing with a butyl rubber septum, and the flask headspace gas was analyzed by GC-TCD every 3 days. After 15 days of incubation, the headspace gas was flushed with 10 mL of pure O_2 or N_2, and then incubation and headspace analysis were continued. To clarify the effect of oxygen concentration on H_2 production by *T. versicolor* K-41, H_2 production experiments under different O_2 concentration conditions were performed. Sealed cedar wood cultures of *T. versicolor* K-41 were prepared as described above. The O_2

concentrations in vials headspace were adjusted to approximately 2.5%, 6.3%, 12.5%, 25% and 50% by O_2 flush, following replacing the headspace gas with pure N_2 gas. After 14 days incubation at 30° C, the headspace gas was analyzed.

Two types of cedar wood meal cultures were prepared (0.5 g of cedar wood meal in a 70-mL serum vial). For the first cultures, 0-1.0% (g/g) $CaCO_3$ was mixed thoroughly with cedar wood meal, and then water was added to adjust the moisture content to 80% before autoclaving. Two PDA discs of *T. versicolor* K-41 were inoculated on the cedar wood meal and then pre-incubated for 5 days at 30°C. After an additional 9 days of incubation with sealing, the headspace gas was analyzed. For the second culture, two PDA discs of *T. versicolor* K-41 were inoculated on wood meal medium without $CaCO_3$ and pre-incubated for 5 days at 30°C. Then, 200 μL of 15 mM (or 0-120 mM) organic acid salt solution (pH 4.5, sodium acetate, formate or oxalate) or water was added to 5 places (40 μL each) in the wood cultures. The vials were then sealed and incubated for an additional 14 days at 30°C, followed by headspace gas analysis.

Two PDA discs of *T. versicolor* K-41 were inoculated in 5 mL of T-medium (2 g/L glucose, 1 g/L yeast extract, 1 g/L KH_2PO_4, 0.2 g/L $[NH_4]_2SO_4$, and 0.5 g/L $MgSO_4{\cdot}7H_2O$ [pH 4.5]) with or without 0.1% $CaCO_3$ in 70-mL serum vials and pre-incubated for 5 days. After 9 days of incubation with sealing, the headspace gas was analyzed in the same manner described above.

2.4 RNA-seq analysis

Cedar wood medium was used for H_2 production, and T-medium was used as a non–H_2-producing medium. *Trametes versicolor* K-41 was incubated aerobically for 10 days on cedar wood medium, and total RNA was extracted from 200 mg (wet) of culture by bead beating in 0.7 mL of Plant RNA Purification Reagent (Invitrogen). The RNA was then purified using an RNeasy Plant Mini kit (Qiagen) plus an RNase-free DNase set (Qiagen) following the manufacturer's protocol. Total RNA was cleaned and concentrated using NucleoSpin RNA Clean-up XS (TaKaRa Bio Inc.) following the manufacturer's protocol. Under non–H_2-producing conditions, 10 mycelial discs were inoculated on 50 mL of T-medium and incubated for 7 days, and total RNA was extracted as described above. RNA quality was assessed by agarose gel electrophoresis and determination of the OD_{260}/OD_{280} ratio.

For RNA-seq analysis, library construction and sequencing were entrusted to Macrogen-Japan Co. The libraries were constructed using a TruSeq Stranded mRNA Library prep kit (Illumina Inc.) according to the manufacturer's protocol. Transcriptome sequencing of paired-end reads (150 bp) was performed using a NovaSeq 6000 system (Illumina). The raw reads (DRR374972-75) were cleaned using Trimomatic v. 0.38 to remove adapter sequences and low-quality bases (quality scores <30) and reads shorter than 100 nt (Bolger et al., 2014). Resultant high-quality paired-end reads were aligned to the *T. versicolor* FP-101664 SS1 genome sequence (GCF_000271585.1) using HISAT2 v. 2.1.0 (Kim et al., 2015). Transcript abundance was estimated using FeatureCounts v. 2.0.0 (Liao et al., 2014). Differentially expressed genes (DEGs) were identified using the likelihood-ratio test implemented in the edgeR package v. 3.16.4 (Robinson et al., 2010). DEGs were defined by a log2 fold-change (logFC) >1 and logFC <−1 with a false discovery rate (FDR) <0.05. To identify significantly over- and under-represented biological features associated with H_2 production, gene ontology (GO) enrichment analysis was performed by parametric analysis of gene set enrichment (Kim and Volsky, 2005) based on the logFC between the H_2-producing and non–H_2-producing conditions.

2.5 Effects of O_2 level and $CaCO_3$ on expression of *Tvhyd* and *Tvfdh*

Trametes versicolor K-41 was pre-incubated for 5-day on cedar wood meal culture with or without 0.5% $CaCO_3$, as described above. After sealing all cultures following removal of PDA pellets, the cultures (without $CaCO_3$) were divided into three groups: O_2 purge (O_2 concentration fitted to average 80%), N_2 purge (O_2 concentration <0.5%), and control (without gas purge). After 7 days of incubation, the headspace gas was analyzed, and total RNA was extracted from 200 mg (wet) of culture. Total RNA (100 ng) was employed for cDNA synthesis using PrimeScript II reverse transcriptase (TaKaRa Bio). Quantitative PCR was performed on a Lightcycler 96 (Roche) system using TB Green Premix Ex Taq II (Tli RNaseH Plus, TaKaRa Bio Inc.). Gene-specific primers for the hydrogenase-like gene (AN: LC710151, *Tvhyd*; 5'-cgcaaatagcacatcgaccg-3'/5'-gacgtgatacac ccactgca-3'), formate dehydrogenase (AN: LC710153, *Tvfdh*; 5'-tact ccgccggaatgaagattgt-3'/5'-aactcatggccctgctcctc-3'), and glyceraldehyde-3-phosphate dehydrogenase (AN: LC710152, *Tvgpd*; 5'-cgctgtgaacgacccccttca-3'/5'-cttgccgtccttgacctcga-3') were designed. Expression levels were calculated according to the ΔΔCq method using *Tvgpd* as the reference gene. Relative H_2 production and expression were calculated by comparison to values of the control.

2.6 Tvfdh expression in *Escherichia coli*

Tvfdh cDNA was amplified to attached *Kpn*I and *Bam*HI sites by PCR using primers (5'-actggtaccatgctcgccggcatctcgtc-3' and 5'-ataggatcctcacttgcgctggccgtacg-3'), then amplified PCR product was ligated between the corresponding restriction sites of pCold I vector (TaKaRa Bio). Constructed vector was transformed into Chaperone Competent Cells pGro7/BL21 (TaKaRa Bio) following manufacture's protocol. The transformed *E. coli* was incubated in 3 mL of LB medium containing 0.5 mg/mL arabinose, 20 μg/mL chloramphenicol and 50 μg/mL ampicillin, at 37 °C, 200 rpm. After OD_{600} was reached at 0.4, the culture was cooled to 4 °C, then 1.0 mM ATP and 0.1 mM isopropyl-β-D-thiogalactopyranoside (IPTG) were added. The culture was incubated for 15 h, at 15 °C, and bacterial cells were recovered by centrifugation (10,000 × *g*, 10 min, 4 °C). Recovered cells were disrupted by bead beating (Micro smash MS-100, Tomy Seiko Co., LTD.), and cell-free extract recovered by addition of 0.1 M NaCl containing 0.1 M Tris-HCl (pH 4.5) was used for FDH activity test. FDH activity was determined by increase in absorbance at 340 nm due to

formation of nicotinamide adenine dinucleotide (NADH) in the reaction mixture (0.75 mL) contained 75 mM potassium phosphate (pH 6.5), 160 μM β-NAD^+, 20 mM sodium formate and 100 μL cell-free extract (Watanabe et al., 2005).

2.7 Construction of pHyg^r and pTvfdh

Restriction sites were attached to *Tvgpd* terminator region by 2 step of PCR reactions, using primers (5'-ggcgcgccag atctgttagcacggagta-3'/5'- gtagattctgtttggtgtgcac-3') for first PCR and (5'-tctagaggatccggcgcgccagatct-3'/5'- gtagattctgtttggtgtgcac-3') for second PCR. The PCR product was TA-cloned into pMD20 vector (TaKaRa Bio), and the resulting plasmid was digested at *Nde*I site. Tagged sequence for In-fusion reaction was attached to *Tvgpd* promoter region by PCR using following primers; 5'-gatctact agtcatactgagatgacctccatagc-3' and 5'-ctctagaaatccatagtggatgtgg tggatgg-3'. The tagged *Tvgpd* promoter was direct cloned into the NedI digested plasmid by In-fusion reaction using In-fusion HD cloning kit (TaKaRa Bio) following manufacture's protocol. The constructed plasmid that having *Asc*I and *Bgl*II sites between *Tvgpd* promoter and terminator regions was designated p*Tvgpd*-pro/ter.

Hygromycin resistant gene (*hyg*^{r}) sequence then was redesigned based on *P. chrysosporium* high-frequency codon usage, and the resulting optimized gene was synthesized by GeneScript Japan, Inc. The *Asc*I and *Bgl*II restriction sites were attached to *hyg*^{r} using primers; ggcgcgccatgaagaagcccgagc and agatctttactccttggcgcgt. p*Tvgpd*-pro/ter was digested by *Asc*I and *Bgl*II. Then the PCR product was ligated into corresponding restriction enzyme sites of p*Tvgpd*-pro/ter (pHyg^r). Tvfdh gene was PCR amplified (primers: 5'-agaggatccggcgcgatgctcgccggcatctcgtc-3'/5'-aacagatctggcg cgtcacttgcgctggccgtacg-3'). The resulting product was used for In-fusion reaction to clone into *Asc*I digested pT*vgpd*-pro/ter to construct plasmid *Tvfdh* is under control of *Tvgpd* promoter (pTvfdh hereafter).

2.8 Homologous recombination of *Tvfdh*

T. versicolor K-41 protoplasts were prepared following method in previous report with some modification. Briefly, *T. versicolor* K-41 was precultured in liquid CYM medium at 30 °C for 7 days. The culture including mycelium was homogenized and 25 ml homogenate was added to 25 mL fresh CYM medium in 500-ml Erlenmeyer flask. The culture was incubated at 30 °C for 3 days, then mycelium was recovered by filtration. Mycelium was resuspended in 0.5M MgOsm (0.5 M $MgSO_4{\cdot}7H_2O$ in 10 mM 2-morpholinoethanesulfonic acid (MES), pH 6.1), following addition of 2 volume of 0.5M MgOsm containing with 5% lysing enzyme (Sigma-Aldrich) and cellulase Onozuka RS (Yakult Pharmaceutical Ind. Co., LTD.). The mixture was incubated at 30 °C, 150 rpm for 16 h. After the reaction, $MgSO_4$ concentration in the solution was adjusted 1.0 M by gently addition of 2.0 M MgOsm. The crude protoplasts solution was layered onto 10 mM MES contained 1.0M sorbitol (SorbOsm), and centrifuged (1,450 × *g*, 15 min, 4 °C) to removed undigested mycelial debris. Protoplasts accumulated on interface were recovered and washed 2 times with SorbOsm. Finally, protoplasts were resuspended in SorbOsm to fit 0.5 to 0.8 × 10^8 cells/mL.

Protoplasts were co-transformed with pHyg^r and pTvfdh. Plasmids (10 μg each) and 40 mM $CaCl_2$ in 300 μL SorbOsm was combined with 500 μL of protoplasts solution. The mixture was incubated for 30 min at 4 °C, and then gently mixed with equal volume of PEG solution (40% PEG #4000, 10 mM $CaCl_2$ in Tris-HCl, pH 7.0). After additional 30 min incubation at 4 °C, the diluted transformation solution with 5mL SorbOsm was mixed with 75 mL of regeneration medium (0.75 M sucrose, 10 mM MES, 0.5% agarose L03 (TaKaRa Bio), 50 μg/mL ampicillin, 20 μg/mL thiabendazole in CYM medium, pH 6.5) at 42 °C, and poured 10 Petri dishes (9 cm diameter). The dishes were incubated at 30 °C for 2 days, 7.5 mL of regeneration medium containing 40 μg/mL hygromycin instead of thiabendazole was overlaid to each dish. Regenerated hyphal clones that appeared in 7 days incubation were picked and subcultured in 20 μg/mL hygromycin containing PDA medium. Genome PCR of regenerated clones were done with specific primers of *Tvfdh* ORF and *Tvgpd* terminator sequences (5'- gagctgctcaagagcttcaag -3'/5'- ggtttcgtttgtggcagagatg-3'), and PCR-positive clones were designated as F1-F38 strains. These transformed strains were employed to experiments, H_2 production from cedar and effect of supplementation of organic acids to H_2 production.

3 Results

3.1 H_2 generation from wood by wood-rot fungi

To investigate the H_2-production activity of wood-rot fungi, 12 strains of wood-rot fungi (K and M strains) isolated from naturally decaying wood were inoculated on beech wood meal. During limited O_2 supply incubation following aerobic cultivation, a small but clear H_2 peak was observed on GC-TCD analysis of the headspace gas of several beech wood meal cultures (Figure 1). H_2 was produced by 8 of 12 tested strains, and classification of those strains was attempted based on the ITS sequences. All 8 strains were found to belong to the Polyporales (1 *Ceriporia* strain, 3 *Phanerochaete* strains, and 4 *Trametes* strains). Therefore, 4 newly described *Trametes* fungi (2 strains each of *T. versicolor* and *T. hirsuta*) and 2 *Phanerochaete* fungi (*P. chrysosporium* and *P. sordida*) were tested in the same way. In addition, an Agaricales fungus (*P. ostreatus*) was also tested as a comparison. Although some strains of Polyporales fungi did not show H_2 production, all strains showing H_2 production belonged to the Polyporales. There were differences in the amount of H_2 produced from beech wood meal among strains of same species.

Nine of the 14 H_2-producing strains were then investigated for H_2 production on cedar wood meal. All tested strains produced H_2 from cedar in amounts greater than produced from beech. Because *T. versicolor* K-41 showed the highest H_2 production level (1.36 μmol/L in headspace gas) in cedar wood meal culture (Figure 1), elucidation of H_2 production mechanism of this fungus was attempted.

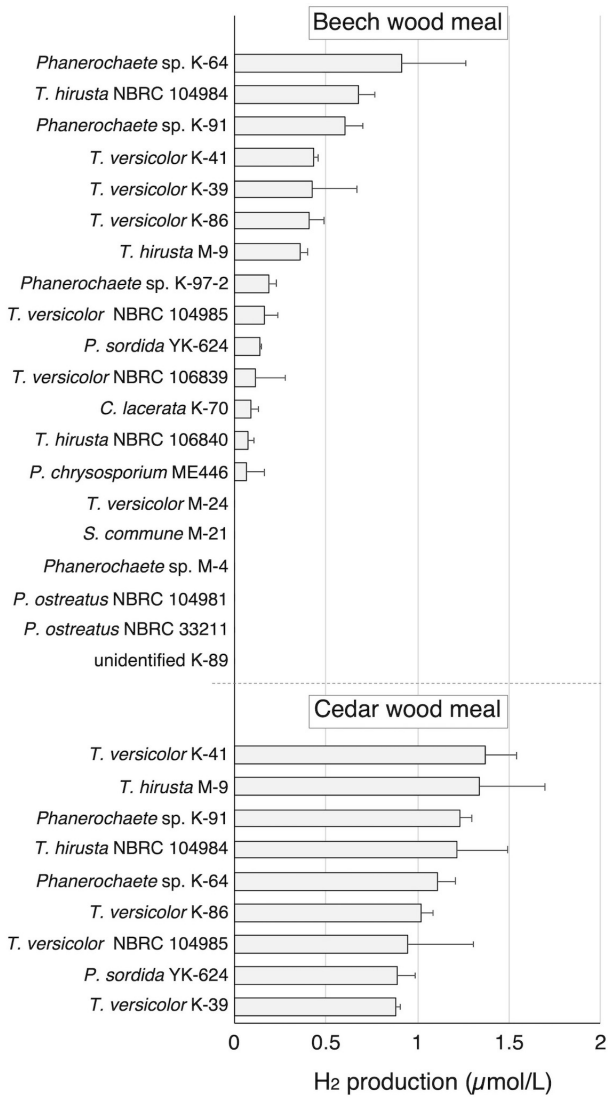

FIGURE 1
H_2 production in beech and cedar wood meal cultures inoculated with white-rot fungi during 14 day incubation with sealing. Values are means ± standard deviation (n=3).

3.2 Characterization of H_2 production activity of *T versicolor* K-41

Time courses of O_2 consumption and H_2 production by cultures of *T. versicolor* K-41 on cedar wood meal during cultivation after sealing were traced and shown in Figure 2. The O_2 concentration in the headspace began to decrease immediately after sealing (Figure 2A). The concentration fell 2.9% by day 12, and thereafter, little O_2 was consumed. By comparison, H_2 production was observed at day 3, and production continued until 12 days of incubation. After termination of H_2 production after 15 days, part of the headspace was replaced with pure O_2 or N_2 gas. Although no effect on H_2 production was observed following replacement with N_2, H_2 production re-started following O_2 replacement (Figure 2B). However, H_2 production stopped again after the O_2 was consumed. Effect initial O_2 concentration on H_2 production is shown in

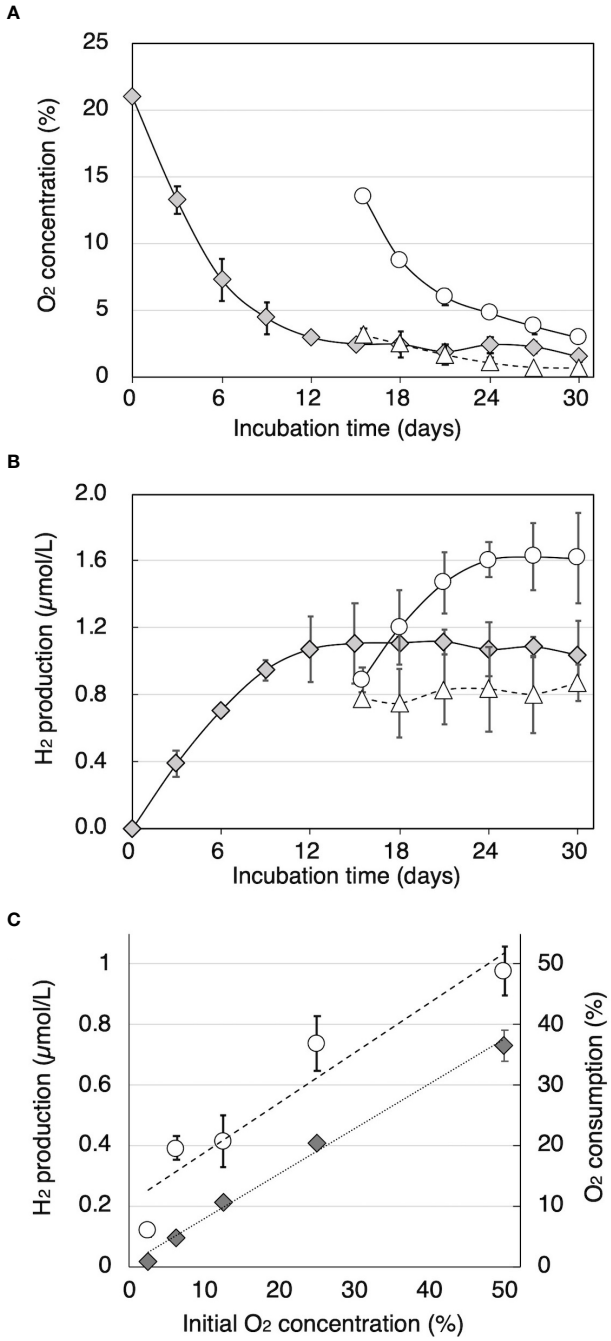

FIGURE 2
The relationship between O_2 concentration and H_2 production in sealed cedar wood meal cultures of *T. versicolor* K-41. Time courses of **(A)** O_2 concentration and **(B)** H_2 concentration in the headspace gas were monitored in sealed cultures (gray diamonds) and cultures flushed with 10 mL of O_2 or N_2 (black circles and white circles, respectively). **(C)** O_2 consumption (black diamonds) and H_2 production (white circles) were measured after 2-week incubation with O_2 and N_2 adjusted to the specified oxygen concentration. The values are the mean ± standard deviation (n=3).

Figure 2C. The result indicated that higher initial O_2 consumption and H_2 production were well correlated with initial O_2 concentration (R2 = 0.983 and 0.863, respectively).

To investigate the relationship between H_2 production and organic acid production during wood decay by *T. versicolor* K-41,

10.3389/ffunb.2023.1201889

H_2 production from cedar wood meal containing 0-1.0% $CaCO_3$ was investigated. It is well known that $CaCO_3$ promotes the production of oxalate and other organic acids generated in the TCA/glyoxylate cycles of basidiomycetes (Takao, 1965). As shown in Figure 3A, *T. versicolor* K-41 showed significantly higher H_2 evolution in cedar meal containing 0.3 and 0.5% $CaCO_3$ than in culture without $CaCO_3$; in particular, 1.5 times higher H_2 production was observed in the culture containing 0.5% $CaCO_3$. Therefore, to clarify involvement of organic acids, oxalate, formate, and acetate were added to 5-day-old cedar wood cultures of *T. versicolor* K-41 just before sealing, and H_2 production was then measured. While no difference was observed in H_2 production between the control and water- or acetate-supplemented cultures, oxalate and formate supplementation increased H_2 production to 120% and 127% compared with the control (Figure 3B). H_2 production increased depending on the level of formate supplementation, reaching a plateau at 6 μmol/flask (Figure 3C). In contrast, no H_2 evolution was observed regardless of $CaCO_3$ addition in T-medium, even though the oxalate and formate concentrations in the medium were increased by $CaCO_3$ addition (Table 1). Thus, H_2 production by *T. versicolor* K-41 may be a specific phenomenon during wood decay and may be related to the metabolism of organic acids, especially formate.

3.3 Estimation of H_2-producing pathway of *T. versicolor*

To identify differences in gene expression between H_2-producing and non–H_2-producing conditions, a differential expression analysis between wood and liquid cultures was performed. These culture conditions were completely different, indicating that gene expression patterns are expected to differ significantly. Simultaneously, it was predicted a possibility of differences in the expression of H_2 production-related genes due to clear differences in H_2 production. Therefore, a differential gene expression analysis under these conditions was conducted. A large number of genes showed differential expression (logFC >1.0 or < −1.0, FDR <0.05); a total of 1,106 and 1,256 genes were up-regulated in wood medium and liquid medium, respectively (Figure 4 and Supplementary Tables 1, 2). In *T. versicolor* K-41 cultivated on wood medium, many genes encoding cellulolytic and ligninolytic enzymes were up-regulated compared with liquid medium (Supplementary Table 1). In contrast, several genes encoding hydrophobin and amylase-type enzymes were down-regulated on wood medium (Supplementary Table 2). GO enrichment analysis indicated that cellulose metabolic process, peroxidase, processes related to oxidative stress, cation uptake, and peptidase activities were over-represented in wood medium (Supplementary Table 3). These results suggest that *T. versicolor* K-41 initiates defensive mechanisms for ROS and radicals generated during the wood decay process.

In the glyoxylate cycle, only the malate synthase gene (XM_008035809.1) was up-regulated on wood medium (Figure 5

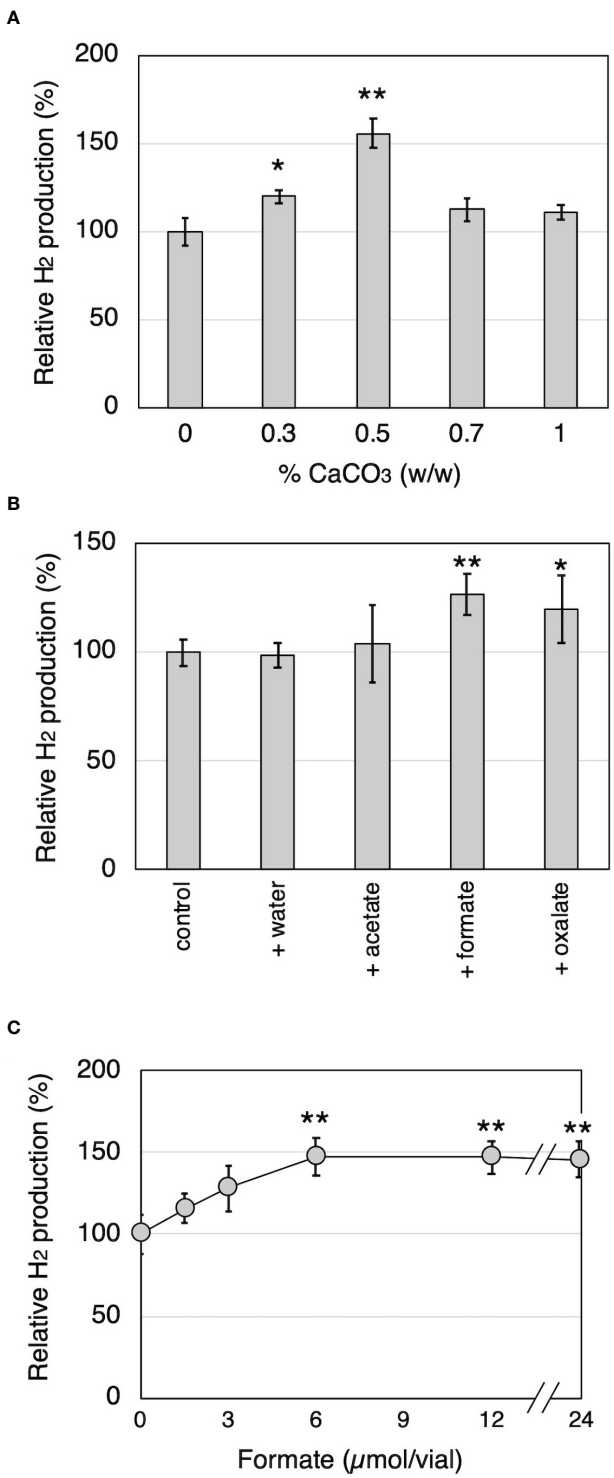

FIGURE 3
The effects of $CaCO_3$ addition and organic acid supplementation on H_2 production by *T. versicolor* K-41 in cedar wood meal cultures. The effects of **(A)** $CaCO_3$ mixed ratio to wood medium, and **(B)** organic acid supplementation prior sealing. **(C)** The relationship between H_2 production and amount of formate added to the wood culture. H_2 production was measured on the 14th day after sealing. Asterisks indicate significant differences compared to the control (without any supplementation, * P<0.05, ** P<0.01). Values are mean ± standard deviation (n=3).

TABLE 1 Cultivation profiles of *T. versicolor* K-41 in liquid medium with or without $CaCO_3$.

	control	0.1% $CaCO_3$
mycelia dry weight (mg)	121.3 ± 2.6	122.6 ± 4.2
oxygen remaining (%)	2.1 ± 0.5	2.2 ± 0.8
organic acid in fluid (mmol/L)		
oxalate	4.4 ± 0.3	10.9 ± 1.6**
formate	0.5 ± 0.1	1.3 ± 0.1 **

The cultures after 14 days incubation with sealing (limiting O2 supply) following 5 days aerobic pre-cultivation were used for the analyses. Asterisks indicate significant differences to wild type or no supplementation control (** P<0.01). Values are means ± standard deviation (n=3).

and Table 2). No induction of TCA cycle (GO:0006099) genes was observed compared with liquid culture, although dehydrogenase E1 and transketolase domain-containing protein 1 (XM_008043731.1) were down-regulated, and succinate dehydrogenase cytochrome b560 subunit (XM_008041764.1) was up-regulated in wood culture (Figure 4, Table 2 and Supplementary Table 3). Malate synthase (XM_008035809.1) of the glyoxylate cycle was up-regulated on wood medium. As shown in Figure 5 and Table 2, possible oxalate-producing enzymes were found in the annotations of the *T. versicolor* FP-101664 SS1 genome: a glyoxylate dehydrogenase (XM_008045016.1) and D- and L-lactate dehydrogenases (XM_008037380.1 and XM_008038286.1) that produce oxalate from glyoxylate (Davies and Asker, 1983; Munir et al., 2001). Although a gene encoding oxalaoacetate, which produces oxalate from oxaloacetate, was not found in the genome, XM_008045015 (annotated as a phosphoenolpyruvate/pyruvate domain-containing protein) showed significant similarity (identity 88.1%, query coverage 86.0%) to the oxaloacetate acetylhydrolase of *Fomitopsis palustris* (accession: AB690578.1, Hisamori et al., 2013). The expression of all of these putative oxalate-producing enzymes in wood culture was clearly lower than the expression in liquid culture. Five oxalate decarboxylase (ODC) genes have been annotated in the *T. versicolor* genome (Table 2). Two of these ODCs were up-regulated (XM_008041462.1 and XM_008041480.1) in wood culture, and two others were down-regulated (XM_008042273.1 and XM_008045068.1). Two highly expressed ODC genes were markedly up-regulated (Figure 4); therefore, all ODC genes appear to be up-regulated. Two formate dehydrogenase (FDH) genes (XM_008035816.1 and XM_008044301.1) showed expression levels ≥4 times higher in wood culture than in liquid culture. The transcript XM_008036235.1, annotated as an iron hydrogenase, showed relatively higher expression in wood culture compared with liquid culture (logFC=0.89, P=0.053, and FDR=0.125).

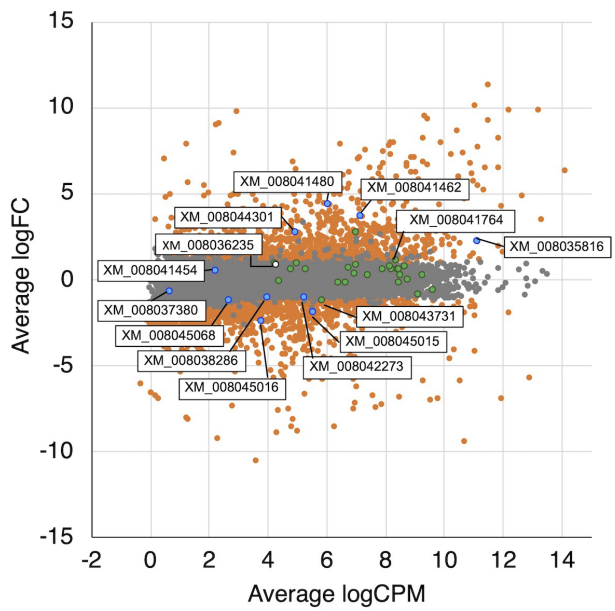

FIGURE 4
MA plot of the normalized data. Each dot represents a single gene, and significantly differentially expressed genes are colored by orange. The genes related TCA/glyoxylate cycle and oxalate metabolism are colored by green and blue, respectively. A white dot is indicated a hydrogenase-like gene.

Tvfdh (encoding a formate dehydrogenase) and *Tvhyd* (annotated as an iron hydrogenase) were identified from the genome and cDNA of *T. versicolor* K-41. Relative production of H_2 and relative expression of *Tvhyd* and *Tvfdh* at 7 days after sealing in N_2- and O_2-purged wood cultures and wood culture containing 0.5% $CaCO_3$ are shown in Figures 6A, B. O_2 purge did not affect H_2 production; however, H_2 was undetectable in N_2-purged cultures (Figure 6A). No difference was observed in H_2 production between the control and O_2-purged samples. This is likely due to the presence of residual O_2 in the samples during the early stages after sealing, resulting in H_2 production still proceeding in both samples. $CaCO_3$ addition increased H_2 production to approximately 150%, as shown in Figure 3A. Relative *Tvhyd* expression was significantly lower (17%) in N_2-purged cultures and higher (172%) in O_2-purged cultures compared with the control. In the case of *Tvfdh*, this gene showed significantly lower expression (less than 1%) in N_2-purged cultures and tended to exhibit lower expression (62%, P=0.051) in O_2-purged cultures. Although there were no significant differences in the expression levels of *Tvhyd* and *Tvfdh* on $CaCO_3$-supplemented cedar culture compared with the control, the expression levels of both genes appeared to be higher. There was a correlation between the *Tvfdh* expression level and H_2 production (r=0.645); therefore, the relationship between *Tvfdh* and H_2 production by *T. versicolor* K-41 was evaluated.

3.4 Effect of self-recombination of *Tvfdh* on H_2 production

Cell-free extract obtained from IPTG-induced *E. coli* retaining *Tvfdh* cDNA in pCold I showed clear NADH formation dependent on formate dehydrogenase activity (data not shown). Thus, construction of *Tvfdh* self-recombinant transformants of *T. versicolor* K-41 was attempted. A total of 38 self-recombinant strains were recovered by co-transformation, and all of these strains were employed to evaluate O_2 consumption during 2

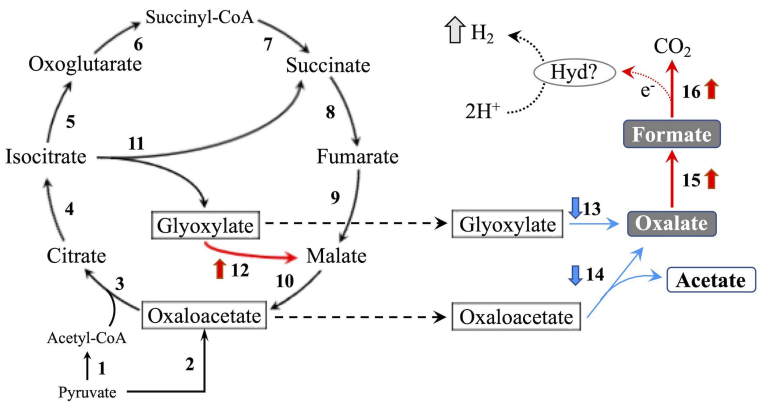

FIGURE 5
TCA/glyoxylate cycle and proposed H_2 production pathway in *T. versicolor* K-41. Numbers beside arrows indicate enzymes catalyzing the reactions; 1: pyruvate dehydrogenase complex, 2: pyruvate carboxylase, 3: citrate synthase, 4: aconitate hydratase, 5: isocitrate dehydrogenase, 6: oxoglutarate dehydrogenase complex, 7: succinate-CoA ligase, 8: succinate dehydrogenase, 9: fumarate hydratase, 10: malate dehydrogenase, 11: isocitrate lyase, 12: malate synthase, 13: glyoxylate dehydrogenase and D/L-lactate dehydrogenase, 14: oxaloacetate acetylhydrolase, 15: oxalate decarboxylase (ODC), and 16: formate dehydrogenase (FDH). Bold upward and downward arrows indicate up- and down-regulated genes in wood culture compared with liquid culture, respectively. Protons may be reduced to H_2 *via* catalytic reaction of an as yet unknown hydrogen-producing enzyme (Hyd)? using electrons produced during formate metabolism.

weeks of incubation on cedar wood meal culture to estimate growth on wood meal. Five transformants showing 50% or higher O_2 consumption were selected. The remaining 33 strains showed approximately 30% or less O_2 consumption, indicating that these strains probably grow slowly on cedar wood medium. The amount of H_2 production and remaining O_2 concentration after 14 days of incubation following sealing of cedar wood cultures inoculated with 5 selected strains were shown in Figure 7A. All selected strains showed a higher amount of H_2 in the headspace. Furthermore, the effect of oxalate and formate supplementation on H_2 production of *Tvfdh* over-expressing strains was investigated (Figure 7B). The wild-type strain exhibited improved H_2 production by the addition of oxalate and formate, and formate supplementation in particular showed a clear effect, as shown in Figure 3. Transformants showed higher H_2 production in cultures with either supplementation than did the wild-type strain with the same supplementation. In contrast, formate supplementation (3 μmol/vial) improved H_2 production by the transformants, whereas oxalate supplementation (3 μmol/vial) did not have a clear effect on H_2 production (Figure 7B).

4 Discussion

Hydrogen and methane gases hold promise as next-generation fuels. Biologically, both gases are produced by anaerobic microorganisms. Recent research revealed that eukaryotes, including animals, plants, and fungi, produce methane during responses to stressors such as ROS, even in the presence of O_2 (Liu et al., 2015). In the case of biohydrogen, many reports have described H_2 production from not only bacteria but also anaerobic eukaryotes. Hydrogenase-like genes are widely distributed among eukaryotes, including higher eukaryotes; however, the functions of these genes are still unknown (Horner et al., 2002). Some reports have described H_2 production by higher plants (e.g., Torres et al., 1986; Jin et al., 2013). Although the physiological roles of H_2 in higher eukaryotes remain unclear, it is thought that H_2 acts as an antioxidant and signaling molecule in higher plants and animals and improves tolerance to ROS (e.g., Itoh et al., 2011; Li et al., 2018). White-rot fungi produce a variety of radicals and ROS during the wood decay process (ten Have and Teunissen, 2001), and they may also have antioxidative self-defense mechanisms.

Based on these observations, it is hypothesized that white-rot fungi produce H_2 as an antioxidant that protects against oxidative stressors such as ROS and radicals that are generated during the wood decay process. In tightly sealed wood cultures, a peak of H_2 on GC analysis was observed in the headspace gas of samples of more than half of the white-rot fungi species tested (Figure 1). While this was a very novel and interesting finding, the respective amounts and efficiencies of H_2 production were less than 1/1000 of bacterial H_2 production from lignocellulose (Ren et al., 2016). Therefore, H_2 production by white-rot fungi during wood decay is likely to be a secondary metabolic reaction rather than primary metabolism associated with energy production. It is possible that a portion of the produced H_2 is consumed to reduce the toxicity of radicals and ROS generated during wood decay under aerobic conditions. The H_2 production properties of *T. versicolor* K-41, which showed the highest H_2 production on wood medium, were thus investigated further. After sealing of the culture vials, this fungus consumed O_2 in the headspace *via* respiration, and H_2 production was only observed during O_2 consumption (Figures 2A, B). If O_2 was re-supplied to the headspace of culture vials after O_2 consumption ceased, the fungus resumed H_2 production. Additionally, H_2 production was well correlated with O_2 concentration (Figure 2C). Thus, these results indicated that white-rot fungi emit H_2 during aerobic respiration but not anaerobic conditions, a property that contrasts markedly with that of bacterial H_2

10.3389/ffunb.2023.1201889

TABLE 2 Fold-change in expression of genes relating to the TCA/glyoxylate cycle and oxalate metabolism in wood culture compared to liquid culture.

Enzyme name[1]/gene ID	Annotation	logFC	logCPM	P value	FDR	GOterm	KOterm
1) Pyruvate dehydrogenase complex							
XM_008037889.1	mitochondrial pyruvate dehydrogenase E1 component beta subunit	0.59	8.23	0.064	0.145		K00161
XM_008034705.1	pyruvate dehydrogenase	0.84	8.14	0.013	0.043		K00627
2) Pyruvate carboxylase							
XM_008040683.1	pyruvate carboxylase	-0.80	9.11	0.016	0.050		K01958
3) Citrate synthase							
XM_008038329.1	citrate synthase-like protein	0.39	6.95	0.184	0.322		K01647
XM_008041170.1	citrate synthase	0.61	8.42	0.057	0.134	GO:0006099	K01647
XM_008040953.1	peroxysomal citrate synthase	0.61	4.78	0.039	0.100	GO:0006099	K01647
4) Aconitate hydratase							
XM_008034216.1	aconitate hydratase	0.95	4.98	0.001	0.006	GO:0006099	K17450
XM_008042398.1	aconitate hydratase	0.27	9.27	0.457	0.613	GO:0006099	K01681
5) Isocitrate dehydrogenase							
XM_008045165.1	isocitrate dehydrogenase	0.92	7.03	0.001	0.006		K00031
XM_008036665.1	hypothetical protein	-0.18	6.66	0.552	0.699	GO:0006099	
XM_008037535.1	hypothetical protein	-0.17	6.40	0.563	0.709	GO:0006099	
6) Oxoglutarate dehydrogenase complex							
XM_008039342.1	2-oxoglutarate dehydrogenase E1 component	-0.11	4.37	0.712	0.825	GO:0006099	K00164
XM_008043264.1	2-oxoglutarate dehydrogenase E1 component	0.06	8.75	0.847	0.918	GO:0006099	K00164
XM_008043731.1	dehydrogenase E1 and transketolase domain-containing protein 1	-1.14	5.87	0.000	0.000	GO:0006099	K15791
XM_008043611.1	dihydrolipoamide succinyltransferase	0.26	7.40	0.362	0.522	GO:0006099	K00658
7) Succinate-CoA ligase							
XM_008033951.1	succinate-CoA ligase	0.70	6.73	0.009	0.032		K01899
XM_008034755.1	succinate-CoA ligase	0.62	7.89	0.043	0.108	GO:0006099	K01900
8) Succinate dehydrogenase							
XM_008037945.1	succinate dehydrogenase	0.31	8.52	0.335	0.494	GO:0006099	K00234
XM_008041764.1	succinate dehydrogenase cytochrome b560 subunit	1.10	8.35	0.001	0.003	GO:0006099	K00236
XM_008043277.1	succinate dehydrogenase iron-sulfur subunit	0.63	8.47	0.051	0.122	GO:0006099	K00235
9) Fumarate hydratase							
XM_008034924.1	fumarate hydratase	-0.17	8.49	0.620	0.754	GO:0006099	K01679
10) Malate dehydrogenase							
XM_008037733.1	malate dehydrogenase	0.82	8.68	0.023	0.068	GO:0006099	K00026
XM_008038723.1	malate dehydrogenase	-0.62	9.61	0.056	0.131	GO:0006099	K00026
11) Isocitrate lyase							
XM_008039384.1	isocitrate lyase	0.58	5.28	0.211	0.356		K01637
XM_008034471.1	isocitrate lyase	0.97	4.23	0.001	0.007		K01637

(Continued)

TABLE 2 Continued

Enzyme name[1]/gene ID	Annotation	logFC	logCPM	P value	FDR	GOterm	KOterm
12) Malate synthase							
XM_008035809.1	malate synthase	2.81	7.03	0.000	0.000	GO:0006097	K01638
13) Oxalate producing enzymes							
XM_008045016.1	glyoxylate dehydrogenase	-2.37	3.80	0.000	0.000		K00101
XM_008037380.1	L-lactate dehydrogenase	-0.71	0.69	0.250	0.402		
XM_008038286.1	D-lactate dehydrogenase cytochrome oxidoreductase	-1.01	3.97	0.000	0.002		K00102
14) Oxaloacetate acetylhydrolase							
XM_008045015.1	Phosphoenolpyruvate/pyruvate domain-containing protein	-1.88	5.54	0.001	0.004		
15) Oxalate decarboxylase (ODC)							
XM_008041454.1	oxalate decarboxylase	0.57	2.26	0.156	0.285	GO:0033609	
XM_008041462.1	oxalate decarboxylase	3.74	7.17	0.000	0.000	GO:0033609	
XM_008041480.1	oxalate decarboxylase	4.45	6.08	0.000	0.000	GO:0033609	
XM_008042273.1	Bicupin oxalate decarboxylase/oxidase	-1.06	5.22	0.001	0.003	GO:0033609	K01569
XM_008045068.1	oxalate decarboxylase	-1.23	2.68	0.001	0.006	GO:0033609	
16) Formate dehydrogenase (FDH)							
XM_008035816.1	NAD-dependent formate dehydrogenase	2.29	11.13	0.000	0.000	GO:0008863	K00122
XM_008044301.1	NAD-dependent formate dehydrogenase	2.79	4.95	0.000	0.001	GO:0008863	K00122
Hyd)? Hydrogenase-like gene							
XM_008036235.1	iron hydrogenase	0.89	4.28	0.053	0.125		

[1] Numerical values in front of gene names are corresponded to Figure 3.

production. These results also suggested that there is a relationship between H_2 production and wood decay by white-rot fungi.

Some H_2-producing bacteria are capable of utilizing short-chain organic acids such as formate, acetate, and lactate for H_2 production (Barbosa et al., 2001; Matsumoto and Nishimura, 2007; McDowall et al., 2014). It has also been shown that hydrogenosomes, organelles found in a wide variety of anaerobic eukaryotes, produce H_2 during pyruvate or malate metabolism (Davidson et al., 2002). These data suggest that organic acids have a significant effect on microbial hydrogen production. In environments with a high C/N ratio, such as wood, it is thought that white-rot fungi dispose of excess carbon as oxalate or other metabolites. Most oxalate is probably produced intracellularly from intermediates (oxaloacetate and glyoxylate) of the TCA and glyoxylic acid cycles (Mäkelä et al., 2002). Although oxalate accumulation in wood culture correlates well with fungal growth and ligninolytic manganese peroxidase activity in some white-rot fungi, including *T. versicolor*, white-rot fungi readily decompose excessive oxalate *via* intra/extracellular metabolism in order to avoid its toxic effect ((Dutton et al., 1993; Mäkelä et al., 2002). Oxalate is degraded to CO_2 *via* formate by intracellular ODC and FDH and also degraded to CO_2 by extracellular peroxidase systems (Shimada et al., 1994). These pathways may enable white-rot fungi to control the concentration of intra/extracellular oxalate to maintain physiological conditions. The concentration of oxalate in the medium was shown to increase after addition of $CaCO_3$ to white-rot fungi cultures (Takao, 1965). The data presented here provide novel insights into the relationship between oxalate metabolism and H_2 production, because higher H_2 production was observed in cedar wood cultures supplemented with $CaCO_3$, oxalate, and formate compared with control cultures (Figures 3, 7). These results suggested that metabolism of organic acids, especially formate, is involved in H_2 production by *T. versicolor* K-41.

No hydrogen production was observed in the liquid culture, even though the addition of $CaCO_3$ enhanced extracellular oxalate accumulation (Table 1). RNA-seq analyses showed that *T. versicolor* K-41 exhibited lower oxalate production and higher oxalate metabolic activity in wood culture compared with liquid culture. As shown in Table 2, *T. versicolor* K-41 promoted the expression of oxalate metabolic enzymes, ODCs and FDHs, in wood culture. In contrast, oxalate-producing enzymes were suppressed. In addition, *T. versicolor* K-41 appeared to avoid accumulation of toxic organic acids, glyoxylate, oxalate, and formate, as only malate synthase was upregulated among the enzymes in the glyoxylate cycle. These result support the hypothesis that oxalate/formate metabolism is involved in H_2 production in wood culture. However, this data did not clarify the relationship between the expression of hydrogenase-like genes and H_2 production by *T. versicolor* K-41. Thus, these experiments indicate that molecular hydrogen synthesis is not the rate-limiting step in the H_2 production system in this fungus.

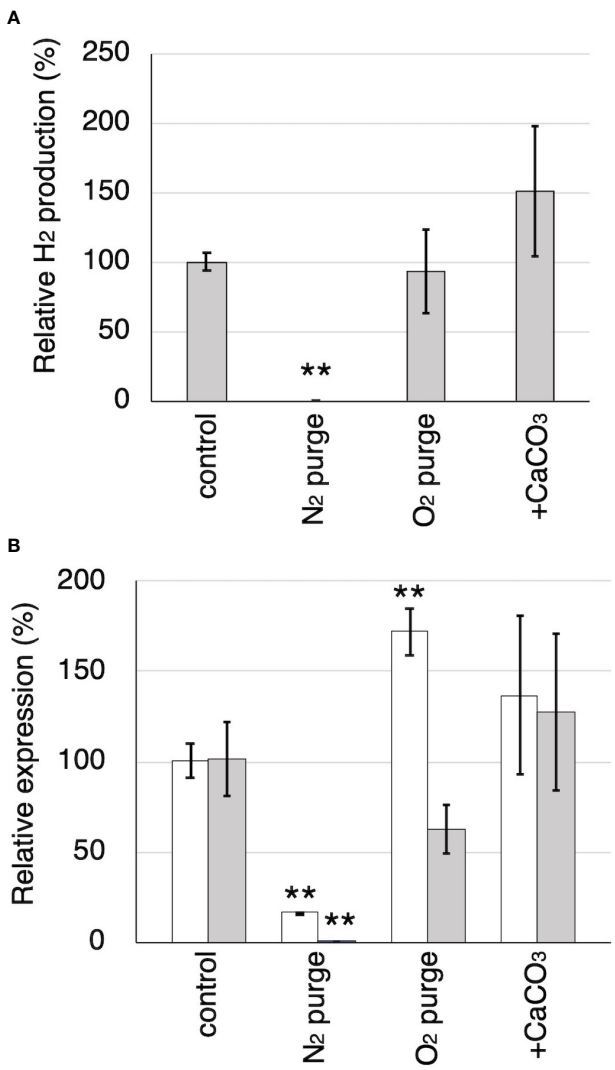

FIGURE 6
The effects of N_2 and O_2 purging, $CaCO_3$ addition to the cultures on H_2 production and the relative expression of *Tvhyd* and *Tvfdh*. **(A)** Relative H_2 production in 7th day compared to the control. **(B)** Relative expression of *Tvhyd* (white) and *Tvfdh* (gray) determined using ΔΔCq method with *Tvgpd* as a reference gene. Asterisks indicate significant differences compared to the control (** *P*<0.01). Values are mean ± standard deviation (n=3).

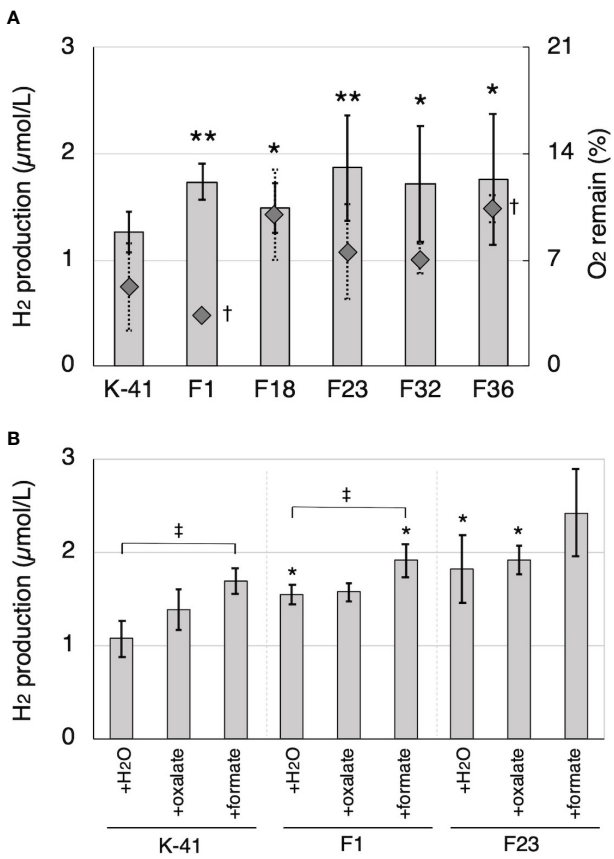

FIGURE 7
H_2 production by *Tvfdh* self-recombination transformants. **(A)** H_2 production and remaining O_2 in cedar wood meal cultures of wild-type strain (K-41) and transformants (F strains). **(B)** The effects of oxalate and formate supplementation to H_2 production of K-41 and transformants. O_2 and H_2 productions were measured on the 14th day after sealing. Asterisks (* and **) indicate significant differences (P<0.05 and 0.01) in H_2 production compared to the wild type (plus same supplementation), respectively. Dagger (†) indicates significant difference in O_2 remaining compared to the wild type (P<0.05). Double dagger (‡) indicates significant difference (P<0.05) compared to the H_2O supplementation control of the same strain. Values are mean ± standard deviation (n=3).

Accordingly, it was investigated the relationship between the expression of a hydrogenase-like gene (*Tvhyd*) and FDH gene (*Tvfdh*) and H_2 production under different O_2 conditions or $CaCO_3$ supplementation (Figure 6). N_2 purge showed clear effects, as low O_2 conditions completely suppressed H_2 production and inhibited *Tvfdh* expression. This result suggests that *Tvfdh* expression is likely more correlated with H_2 production than *Tvhyd*. Therefore, formate metabolism catalyzed by TvFDH is probably involved in H_2 production. *Tvfdh* self-recombination strains that maintained O_2 consumption produced higher amounts of H_2 in the headspace than the wild-type strain; however, transformants only exhibited improved H_2 production following formate supplementation, unlike the wild type (Figure 7). These results suggest that the amounts of oxalate and formate or the associated metabolic activities are the rate-limiting step in H_2 production by *T. versicolor* K-41. Therefore, a possible H_2 production pathway for *T. versicolor* K-41 is proposed, as shown in Figure 5. Oxalate originating in the TCA/glyoxylate cycle is metabolized to form formate by intracellular ODC, and FDH oxidized formate to generate CO_2, H^+, and two electrons. from formate. Then, TvHYD or an as yet unknown hydrogenase perhaps produces H_2 from protons by utilizing electrons produced in formate metabolism.

In this study, it was discovered that some white-rot fungi belonging to the Polyporales are capable of producing H_2 during wood decay. In the case of *T. versicolor* K-41, which showed the highest H_2 production, the fungus produced H_2 under aerobic conditions, and oxalate/formate metabolism is likely linked to the H_2 production system. In addition to these results, self-recombination of *Tvfdh* clearly improved H_2 production in cedar wood culture, thus suggesting that TvFDH is involved in H_2

production by this fungus. This novel finding of aerobic H_2 production by an aerobic white-rot fungus opens new areas of inquiry in biohydrogen research. It is expected that be economically advantageous over anaerobic fermentation for process control if an aerobic H_2 production process could be established. However, the current H_2 production by white rot fungi is far below the commercially viable level. Additionally, there are many open questions remaining in terms of the mechanism of aerobic H_2 production by white-rot fungi, the involvement of bacterial symbionts in H_2 production by white-rot fungi has not been excluded, and the H_2 production mechanism remains unclear. In future studies, identification of the enzyme producing H_2 and the underlying mechanism will be attempted in order to shed light on the physiological function of H_2 production in white-rot fungi.

Data availability statement

The datasets presented in this study can be found in the DDBJ repository, accession number DRA014108 (https://ddbj.nig.ac.jp/resource/sra-submission/DRA014108).

Author contributions

TM screened H_2-producing fungi, analyzed gene expression, interpreted experiments, and wrote the manuscript. ST analyzed the effect of oxygen and self-recombinant strains. AS performed characterization of H_2 production activity. MA determined gene and cDNA sequences and contributed screening. RK and YY contributed to the construction of recombinant strains. HD performed RNA-seq and analyzed the data. HK proposed the H_2 production pathway. HH designed and interpreted the experiments and wrote the manuscript. All authors contributed to the article and approved the submitted version.

Funding

This work was supported by Japan Society for the Promotion of Science Grants-in-Aid for Scientific Research (KAKENHI), grant numbers JP16K15074 and JP18H02311.

Conflict of interest

The authors declare that the research was conducted in the absence of any commercial or financial relationships that could be construed as a potential conflict of interest.

Publisher's note

All claims expressed in this article are solely those of the authors and do not necessarily represent those of their affiliated organizations, or those of the publisher, the editors and the reviewers. Any product that may be evaluated in this article, or claim that may be made by its manufacturer, is not guaranteed or endorsed by the publisher.

Supplementary material

The Supplementary Material for this article can be found online at: https://www.frontiersin.org/articles/10.3389/ffunb.2023.1201889/full#supplementary-material

References

Azwar, M. Y., Hussain, M. A., and Abdul-Wahab, A. K. (2014). Development of biohydrogen production by photobiological, fermentation and electrochemical processes: a review. *Renew. Sustain. Energy Rev.* 31, 158–173. doi: 10.1016/j.rser.2013.11.022

Barbosa, M. J., Rocha, J. M. S., Tramper, J., and Wijffels, H. R. (2001). Acetate as a carbon source for hydrogen production by photosynthetic bacteria. *J. Biotechnol.* 85, 25–33. doi: 10.1016/S0168-1656(00)00368-0

Bolger, A. M., Lohse, M., and Usadel, B. (2014). Genome analysis Trimmomatic: a flexible trimmer for illumina sequence data. *Bioinfomatics* 30, 2114–2120. doi: 10.1093/bioinformatics/btu170

Dashtban, M., Schraft, H., Syed, T. A., and Qin, W. (2010). Fungal biodegradation and enzymatic modification of lignin. *Int. J. Biochem. Mol. Biol.* 1, 36–50.

Davidson, E. A., van der Giezen, M., Horner, D. S., Embley, T. M., and Howe, C. J. (2002). An [Fe] hydrogenase from the anaerobic hydrogenosome-containing fungus neocallimastix frontalis L2. *Gene* 296, 45–52. doi: 10.1016/S0378-1119(02)00873-9

Davies, D. D., and Asker, H. (1983). Synthesis of oxalic acid by enzymes from lettuce leaves. *Plant Physiol.* 72, 134–138. doi: 10.1104/pp.72.1.134

Dutton, M. V., Evans, C. S., Atkey, P. T., and Wood, D. A. (1993). Oxalate production by basidiomycetes, including the white-rot species coriolus versicolor and phanerochaete chrysosporium. *Appl. Microbiol. Biotechnol.* 39, 5–10. doi: 10.1007/BF00166839

Ghimire, A., Frunzo, L., Pirozzi, F., Trably, E., Escudie, R., Lens, P. N. L., et al. (2015). A review on dark fermentative biohydrogen production from organic biomass: process parameters and use of by-products. *Appl. Energy* 144, 73–95. doi: 10.1016/j.apenergy.2015.01.045

Hackstein, J. H. P., Akhmanova, A., Boxma, B., Harhangi, H. R., and Voncken, F. G. J. (1999). Hydrogenosomes: eukaryotic adaptations to anaerobic environments. *Trends Microbiol.* 7, 441–447. doi: 10.1016/S0966-842X(99)01613-3

Hess, M., Paul, S. S., Puniya, A. K., Giezen, M., Shaw, C., Edwards, J. E., et al. (2020). Anaerobic fungi: past, present, and future. *Front. Microbiol.* 11. doi: 10.3389/fmicb.2020.584893

Hisamori, H., Watanabe, T., Suzuki, S., Okawa, K., Sakai, H., Yoshimura, T., et al. (2013). Cloning and expression analysis of a cDNA encoding an oxaloacetate acetylhydrolase from the brown-rot fungus fomitopsis palustris. *Sustain. Humanosph.* 9, 57–64.

Horner, D. S., Heil, B., Happe, T., and Embley, T. M. (2002). Iron hydrogenases - ancient enzymes in modern eukaryotes. *Trends Biochem. Sci.* 27, 148–153. doi: 10.1016/S0968-0004(01)02053-9

Itoh, T., Hamada, N., Terazawa, R., Ito, M., Ohno, K., Ichihara, M., et al. (2011). Molecular hydrogen inhibits lipopolysaccharide / interferon γ-induced nitric oxide production through modulation of signal transduction in macrophages. *Biochem. Biophys. Res. Commun.* 411, 143–149. doi: 10.1016/j.bbrc.2011.06.116

Jin, Q., Zhu, K., Cui, W., Xie, Y., Han, B., and Shen, W. (2013). Hydrogen gas acts as a novel bioactive molecule in enhancing plant tolerance to paraquat-induced oxidative stress *via* the modulation of heme oxygenase-1 signalling system. *Plant Cell Environ.* 36, 956–969. doi: 10.1111/pce.12029

Kim, D., Langmead, B., and Salzberg, S. L. (2015). HISAT: a fast spliced aligner with low memory requirements. *Nat. Methods* 12, 357–360. doi: 10.1038/nmeth.3317

Kim, S. Y., and Volsky, D. J. (2005). PAGE: parametric analysis of gene set enrichment. *BMC Bioinf.* 6, 144. doi: 10.1186/1471-2105-6-144

Li, C., Gong, T., Bian, B., and Liao, W. (2018). Roles of hydrogen gas in plants: a review. *Funct. Plant Biol.* 45, 783–792. doi: 10.1071/FP17301

Liao, Y., Smyth, G. K., and Shi, W. (2014). FeatureCounts: an efficient general purpose program for assigning sequence reads to genomic features. *Bioinformatics* 30, 923–930. doi: 10.1093/bioinformatics/btt656

Liu, J., Chen, H., Zhu, Q., Shen, Y., Wang, X., Wang, M., et al. (2015). A novel pathway of direct methane production and emission by eukaryotes including plants, animals and fungi: an overview. *Atmos. Environ.* 115, 26–35. doi: 10.1016/j.atmosenv.2015.05.019

Mäkelä, M., Galkin, S., Hatakka, A., and Lundell, T. (2002). Production of organic acids and oxalate decarboxylase in lignin-degrading white rot fungi. *Enzyme Microb. Technol.* 30, 542–549. doi: 10.1016/S0141-0229(02)00012-1

Marvin-Sikkema, F. D., Gomes, T. M. P., Grivet, J.-P., Gottschal, J. C., and Prins, R. A. (1993). Characterization of hydrogenosomes and their role in glucose metabolism of neocallimastix sp. L2. *Arch. Microbiol.* 160, 388–396. doi: 10.1007/BF00252226

Matsumoto, M., and Nishimura, Y. (2007). Hydrogen production by fermentation using acetic acid and lactic acid. *J. Biosci. Bioeng.* 103, 236–241. doi: 10.1263/jbb.103.236

McDowall, J. S., Murphy, B. J., Haumann, M., Palmer, T., Armstrong, F. A., and Sargent, F. (2014). Bacterial formate hydrogenlyase complex. *Proc. Natl. Acad. Sci. U.S.A.* 111, E3948–E3956. doi: 10.1073/pnas.1407927111

Mnatsakanyan, N., Bagramyan, K., and Trchounian, A. (2004). Hydrogenase 3 but not hydrogenase 4 is major in hydrogen gas production by escherichia coli formate hydrogenlyase at acidic pH and in the presence of external formate. *Cell Biochem. Biophys.* 41, 357–365. doi: 10.1385/CBB:41:3:357

Mori, T., Kako, H., Sumiya, T., Kawagishi, H., and Hirai, H. (2016). Direct lactic acid production from beech wood by transgenic white-rot fungus phanerochaete sordida YK-624. *J. Biotechnol.* 239, 83–89. doi: 10.1016/j.jbiotec.2016.10.014

Mori, T., Sudo, S., Kawagishi, H., and Hirai, H. (2018). Biodegradation of diuron in artificially contaminated water and seawater by wood colonized with the white-rot fungus trametes versicolor. *J. Wood Sci.* 64, 690–696. doi: 10.1007/s10086-018-1740-x

Munir, E., Yoon, J. J., Tokimatsu, T., Hattori, T., and Shimada, M. (2001). A physiological role for oxalic acid biosynthesis in the wood-rotting basidiomycete fomitopsis palustris. *Proc. Natl. Acad. Sci. U.S.A.* 98, 11126–11130. doi: 10.1073/pnas.191389598

Ohta, S. (2012). Molecular hydrogen is a novel antioxidant to ef fi ciently reduce oxidative stress with potential for the improvement of mitochondrial diseases. *Biochmica Biophys. Acta* 1820, 586–594. doi: 10.1016/j.bbagen.2011.05.006

Ren, N. Q., Zhao, L., Chen, C., Guo, W. Q., and Cao, G.-L. (2016). A review on bioconversion of lignocellulosic biomass to H2: key challenges and new insights. *Bioresour. Technol.* 215, 92–99. doi: 10.1016/j.biortech.2016.03.124

Renwick, G. M., Giumarro, C., and Siegel, S. M. (1964). Hydrogen metabolism in higher plants. *Plant Physiol.* 39, 303–306. doi: 10.1104/pp.39.3.303

Robinson, M. D., McCarthy, D. J., and Smyth, G. K. (2010). edgeR: a bioconductor package for differential expression analysis of digital gene expression data. *Bioinformatics* 26, 139–140. doi: 10.1093/bioinformatics/btp616

Shimada, M., Ma, D. B., Akamatsu, Y., and Hattori, T. (1994). A proposed role of oxalic acid in wood decay systems of wood-rotting basidiomycetes. *FEMS Microbiol. Rev.* 13, 285–295. doi: 10.1111/j.1574-6976.1994.tb00049.x

Takao, S. (1965). Organic acid production by basidiomycetes, i. screening of acid-producing strains. *Appl. Microbiol.* 13, 732–737. doi: 10.1128/am.13.5.732-737.1965

ten Have, R., and Teunissen, P. J. M. (2001). Oxidative mechanisms involved in lignin degradation by white-rot fungi. *Chem. Rev.* 101, 3397–3413. doi: 10.1021/cr000115l

Torres, V., Ballesteros, A., and Fernández, V. M. (1986). Expression of hydrogenase activity in barley (hordeum vulgare l.) after anaerobic stress. *Arch. Biochem. Biophys.* 245, 174–178. doi: 10.1016/0003-9861(86)90202-X

Watanabe, T., Hattori, T., Tengku, S., and Shimada, M. (2005). Purification and characterization of NAD- dependent formate dehydrogenase from the white-rot fungus Ceriporiopsis subvermispora and possible role of the enzyme in oxalate metabolism. *Microb. Technol.* 27, 68–75. doi: 10.1016/j.enzmictec.2005.01.032

Xie, Y., Mao, Y., Lai, D., Zhang, W., and Shen, W. (2012). H2 enhances arabidopsis salt tolerance by manipulating ZAT10 / 12-mediated antioxidant defence and controlling sodium exclusion. *PloS One* 7, e49800. doi: 10.1371/journal.pone.0049800

Zeng, J., Zhang, M., and Sun, X. (2013). Molecular hydrogen is involved in phytohormone signaling and stress responses in plants. *PloS One* 8, e71038. doi: 10.1371/journal.pone.0071038